

UC Davis

UC Davis Previously Published Works

Title

Rad51 paralogues Rad55–Rad57 balance the antirecombinase Srs2 in Rad51 filament formation

Permalink

<https://escholarship.org/uc/item/0vc666tt>

Journal

Nature, 479(7372)

ISSN

0028-0836

Authors

Liu, Jie
Renault, Ludovic
Veaute, Xavier
[et al.](#)

Publication Date

2011-11-01

DOI

10.1038/nature10522

Peer reviewed



HHS Public Access

Author manuscript

Nature. Author manuscript; available in PMC 2012 May 10.

Published in final edited form as:

Nature. ; 479(7372): 245–248. doi:10.1038/nature10522.

Rad51 paralogs Rad55-Rad57 balance the anti-recombinase Srs2 in Rad51 filament formation

Jie Liu¹, Ludovic Renault², Xavier Veaute³, Francis Fabre³, Henning Stahlberg^{2,4}, and Wolf-Dietrich Heyer^{1,2,#}

¹Department of Microbiology, University of California at Davis, Davis, CA95616-8665, USA

²Department of Molecular & Cellular Biology, University of California at Davis, Davis, CA95616-8665, USA ³CEA–DSV-Institut de Radiobiologie Cellulaire et Moléculaire, UMR217 CNRS/CEA, F-92265 Fontenay aux Roses, France ⁴Center for Cellular Imaging and Nanoanalytics, University Basel, CH-4056 Basel, Switzerland

Abstract

Homologous recombination is a high-fidelity DNA repair pathway. Besides a critical role in accurate chromosome segregation during meiosis, recombination functions in DNA repair and in the recovery of stalled or broken replication forks to ensure genomic stability. In contrast, inappropriate recombination contributes to genomic instability, leading to loss of heterozygosity, chromosome rearrangements, and cell death. The RecA/UvsX/RadA/Rad51 family of proteins catalyzes the signature reactions of recombination, homology search and DNA strand invasion^{1,2}. Eukaryotes also possess Rad51 paralogs, whose exact role in recombination remains to be defined³. Here we show that the budding yeast Rad51 paralogs, the Rad55-Rad57 heterodimer, counteract the anti-recombination activity of the Srs2 helicase. Rad55-Rad57 associate with the Rad51-ssDNA filament, rendering it more stable than a nucleoprotein filament containing Rad51 alone. The Rad51/Rad55-Rad57 co-filament resists disruption by the Srs2 anti-recombinase by blocking Srs2 translocation involving a direct protein interaction between Rad55-Rad57 and Srs2. Our results demonstrate an unexpected role of the Rad51 paralogs in stabilizing the Rad51 filament against a biologically important antagonist, the Srs2 anti-recombination helicase. The biological significance of this mechanism is indicated by a complete suppression of the ionizing radiation sensitivity of *rad55* or *rad57* mutants by concomitant deletion of *SRS2*, as expected for biological antagonists. We propose that the Rad51 presynaptic filament is a meta-stable reversible intermediate, whose assembly and disassembly is governed by the balance between Rad55-Rad57 and Srs2, providing a key regulatory mechanism controlling the initiation of homologous

Users may view, print, copy, download and text and data- mine the content in such documents, for the purposes of academic research, subject always to the full Conditions of use: http://www.nature.com/authors/editorial_policies/license.html#terms

Correspondence and requests for material should be addressed to Wolf-Dietrich Heyer Tel. (530) 752-3001, FAX (530) 752-3011. wdhey@ucdavis.edu.

Full methods and any associated references are available in the online version of the paper at www.nature.com/nature

Author contribution: J.L. designed, performed, analyzed all experiments, except the IR survival assay, and helped write the manuscript. L.R. helped with the EM image collection and data analysis. X.V. purified Srs2 protein. F.F. performed the IR experiment. H.S. advised on the EM analysis. W.D.H. conceived the project, designed experiments, coordinated collaborations, contributed to data analysis and wrote the manuscript. All authors discussed results and edited the manuscript.

The authors declare no competing financial interests.

recombination. These data provide a paradigm for the potential function of the human RAD51 paralogs, which are known to be involved in cancer predisposition and human disease.

Rad51 protein and its homologs RecA, UvsX, and RadA form nucleoprotein filaments with ssDNA that perform homology search and DNA strand invasion during homologous recombination. The Rad51 paralogs share the RecA core with the Rad51 protein featuring unique N- and C-terminal extensions (Supplementary Fig. 2), but themselves do not form filaments and are unable to perform homology search and DNA strand invasion²⁻⁴. While humans contain five paralogs (RAD51B, RAD51C, RAD51D, XRCC2, XRCC3), the budding yeast *Saccharomyces cerevisiae* contains two clearly identifiable paralogs, Rad55 and Rad57 (Supplementary Fig. 2). Rad55 and Rad57 in yeast as well as the five human RAD51 paralogs have unique non-redundant functions in recombination, and mutations in any one of them lead to recombination defects, chromosomal instability, sensitivity to DNA damage, and meiotic defects¹⁻³. Defects in the budding yeast *RAD55* and *RAD57* genes lead to identical and epistatic phenotypes in DNA repair and recombination, consistent with the formation of a stable Rad55-Rad57 heterodimer^{4,5}. Rad55-Rad57 were inferred to function as mediator proteins (ref. ⁶) allowing assembly of the Rad51 nucleoprotein filament on ssDNA covered by the eukaryotic ssDNA-binding protein RPA⁴. This suggested that Rad55-Rad57 are involved in the nucleation of the Rad51 filament, which is otherwise inhibited on RPA-covered ssDNA. This nucleation model is akin to the role of RecFOR or BRCA2 in nucleating RecA or human RAD51 filaments⁷⁻⁹. Rad51 filament formation *in vivo* can be monitored cytologically as Rad51 focus formation at the site of DNA damage¹⁰. Unexpectedly, Rad51 focus formation after IR in yeast was demonstrated to be independent of Rad55-Rad57 and formation of visible Rad55-Rad57 foci required Rad51¹⁰. These results are difficult to reconcile with the nucleation model derived from the biochemical results and suggest an alternative function of Rad55-Rad57 *in vivo*.

To address the function of the Rad51 paralogs in yeast, we determined the effect of Rad55-Rad57 on the stability of Rad51-ssDNA nucleoprotein complexes. Deletion mutants of the *RAD55* or *RAD57* genes display a curious enhancement of some phenotypes at low temperature (in particular IR sensitivity; see Supplementary Fig. 12)⁵, suggesting that these proteins are involved in the stabilization of a molecular complex, likely the Rad51 presynaptic filament. To test this hypothesis, we incubated subsaturating amounts of Rad51 protein with ssDNA (1 Rad51 per 15 nts) in the presence of substoichiometric amounts of Rad55-Rad57 heterodimer (1 Rad55-Rad57 per 4 Rad51) and challenged the filaments with buffer containing high salt (500 mM NaCl) (Supplementary Fig. 3a, b). Under these conditions, Rad51 does not maintain stable complexes with ssDNA during electrophoresis. However, the presence of Rad55-Rad57 resulted in stable, Rad51-containing ssDNA complexes that withstood the salt challenge. In a complementary approach, we examined the effect of Rad55-Rad57 on Rad51 filament formation at near physiological ionic strength (90 mM NaCl) (Fig. 1a, b). Under these conditions, only a fraction of the available Rad51 binds ssDNA, causing retarded mobility of the DNA (Fig. 1b, lane 3). Addition of substoichiometric amounts of Rad55-Rad57 (1 Rad55-Rad57 per 6 Rad51 in lane 4 of Fig. 1b) led to the formation of a novel, supershifted complex that contained both Rad51 and Rad55-Rad57, as demonstrated by immunoblotting. Rad55-Rad57 alone binds to DNA

under these conditions, leading to the formation of protein-networks that are too large to enter the gel (Fig. 1b, lane 2). The results from both experiments (Fig. 1b; Supplementary Fig. 3) suggest that Rad55-Rad57 form a co-complex with Rad51 on ssDNA and stabilize Rad51-ssDNA filaments. Indeed, immunogold electron microscopy (EM) targeted towards Rad55 (GST-tag; see Fig. 1c) directly visualized Rad55 associated with the Rad51-ssDNA filaments (Fig. 1d). Control experiments demonstrated the specificity of the gold labeling (Supplementary Table 1) with over 90% of the gold particles associated with clearly identifiable Rad51 filaments. The remainder may have associated with filaments too short to be scored or with free Rad55-Rad57. Gold particles were found either at the filament terminus (n=40) or interstitially (n=43) (Supplementary Table 1). Negative controls with Rad51 filaments assembled in the absence of Rad55-Rad57 showed negligible gold labeling (Supplementary Table 1). These data show that Rad55-Rad57 are associated with the Rad51-ssDNA filament, but the exact disposition of the heterodimer with the filament remains to be determined (see Fig. 1e).

Salt stability of protein-DNA complexes is a valuable biochemical criterion. To establish biological significance, we tested whether Rad55-Rad57 stabilize Rad51-ssDNA filaments against a biologically relevant destabilizer. The Srs2 helicase was identified as a negative regulator of homologous recombination, and genetic experiments suggested that Srs2 targets Rad51 protein¹¹⁻¹³. Consistent with the genetic data, Srs2 translocates on ssDNA and disrupts Rad51 presynaptic filaments *in vitro*, providing a compelling mechanism for its function as an anti-recombinase¹⁴⁻¹⁶. In the presence of 0.1 or 0.33 μM Srs2 approximately 70% of the Rad51 is dissociated as assessed by measuring Rad51 associated with ssDNA coupled to magnetic beads (Fig. 2a- c). The presence of substoichiometric amounts of Rad55-Rad57 (0.1 μM) enhanced the recovery of ssDNA-bound Rad51 by ~ 2 -fold (from 31% to 60% in the presence of 333 nM Srs2). Rad55-Rad57 and Srs2 bound to Rad51-covered ssDNA in a quantitative and concomitant manner (Fig. 2d). Together the data show that Rad55-Rad57 inhibit Srs2 when bound to DNA and not in solution. Concentration-dependent inhibition of Srs2-mediated dissociation of Rad51 from ssDNA by Rad55-Rad57 was also observed in a topology-based assay (Supplementary Fig. 4, 5).

To further investigate the role of Rad55-Rad57 in antagonizing disruption of Rad51 presynaptic filaments by Srs2, we utilized EM to examine nucleoprotein filaments directly (Fig. 3; Supplementary Fig. 6). Rad51 filaments were assembled on a 600 nt fragment of ssDNA and RPA was added to visualize free ssDNA. Consistent with previous observations^{14,15}, in the absence of Rad55-Rad57 Srs2 disrupts the Rad51-ssDNA filament efficiently, leading to binding of RPA to the newly exposed ssDNA (Fig. 3). Importantly, when sub-stoichiometric amounts of Rad55-Rad57 were co-incubated with Rad51 and ssDNA, the filaments were stabilized against disruption by Srs2, as indicated by the significantly increased mean filament length.

How do Rad55-Rad57 block Srs2 from dissociating Rad51 from ssDNA? Srs2 is known to interact with Rad51 and trigger the Rad51 ATPase leading to dissociation of Rad51 from ssDNA¹⁶. We found that Rad55-Rad57 form a 1:1 complex with Srs2 (Fig. 4a) and have higher affinity to Srs2 than to Rad51 (Fig. 4b, c). Excess Rad51 does not compete with Srs2 binding to Rad55-Rad57 (Supplementary Fig. 7). Moreover, Rad55-Rad57 are able to

simultaneously bind Rad51 and Srs2 in a 1:1:1 stoichiometry (Fig. 4d; Supplementary Figs. 7-9). We entertained the possibility that Rad55-Rad57 inhibit the Srs2 ATPase activity and by that Srs2 translocation, but Srs2 ATPase activity is barely altered by the presence of Rad55-Rad57 (data not shown). Srs2 translocase/helicase activity is stimulated by Rad51 binding to DNA¹⁷ (Fig. 4e-g). Importantly, Rad55-Rad57 completely suppress this stimulatory effect of Rad51, leading to inhibition of the Srs2 helicase activity even at a 5-fold molar excess of Srs2 over Rad55-Rad57 (Fig. 4f, g; Supplementary Fig. 10). This substoichiometric action of Rad55-Rad57 eliminates the possibility that Rad55-Rad57 inhibition functions by binding Srs2 in solution. Rad55-Rad57 only slightly inhibit Srs2 helicase in the absence of Rad51 (Fig. 4g; Supplementary Fig. 10c). Control experiments show that this effect depends on Srs2 translocating in the expected 3' to 5' direction (Supplementary Fig. 10d), showing that Rad55-Rad57 inhibit Srs2 translocation on DNA to increase filament stability (Figs. 1, 2) and function (Supplementary Fig. 11). Direct visualization of human RAD51 filaments revealed that RAD51 is only able to form discontinuous short clusters on dsDNA, as a result of frequent nucleation but limited extension^{18,19}. If this property holds true for ssDNA, the formation of a co-filament with Rad51 by Rad55-Rad57 might provide a mechanism to form extended Rad51 filaments. This could also explain the increase in Rad55-Rad57 focus intensity over time in following IR exposure and is consistent with the dependence of Rad55-Rad57 foci on Rad51¹⁰.

Our biochemical data are consistent with a model (Supplementary Fig. 1) whereby Rad51 presynaptic filament formation is modulated by a balance between the stabilizing function of Rad55-Rad57 and the destabilizing function of Srs2 anti-recombinase. This model predicts that a deletion of *SRS2* should suppress the phenotypes caused by defects in Rad55-Rad57. In fact, *srs2* completely suppresses the IR sensitivity of *rad57* and *rad55* mutations in quantitative survival assays (Supplementary Fig. 12), consistent with semi-quantitative results using *rad57*²⁰. However, *srs2* only mildly suppresses the MMS sensitivity (Supplementary Fig. 13) and recombination defect (Supplementary Fig. 14) of a *rad55* mutation, consistent with previous *rad57* data²⁰. The difference in suppression is likely related to that IR-induced DNA damage requires primarily DSB repair, whereas MMS-induced DNA damage and sister chromatid recombination require gap repair (Supplementary Fig. 1). We propose that the Rad51 presynaptic filament is a meta-stable reversible intermediate, whose dynamics in yeast are partially controlled by the balance of the filament-stabilizing activity of Rad55-Rad57 and the filament-destabilizing activity of the Srs2 helicase (Supplementary Fig. 1). This balance is likely influenced by the multiple post-translational modifications that have been identified to regulate Rad55-Rad57²¹ and Srs2²² functions (Supplementary Fig. 1) (ref. ¹). Together with the local availability of SUMO-PCNA, which specifically recruits Srs2²³⁻²⁵, post-translational modifications may determine the balance between recombination and anti-recombination in wild type cells and explain the various degrees of suppression observed in the *srs2 rad55 (rad57)* double mutants that depend on the type of DNA damage or genetic endpoint (DSB *versus* replication fork associated gap in Supplementary Fig. 1).

The human RAD51 paralogs play important roles in tumor suppression and human disease^{3,26}. Our studies established an unprecedented mechanism of anti-antirecombination

that may serve as a paradigm for the mechanism of action of the five human RAD51 paralogs. The diversification of the human RAD51 paralogs may reflect the multiplicity of human motor proteins that may disrupt RAD51 presynaptic filaments, including the RecQ-like helicases BLM and RECQL5 as well as FBH1 and FANCD1²⁷⁻³⁰ or indicate additional functions during recombinational repair.

Methods summary

Purification of yeast Rad51, Rad55-Rad57, RPA, and Srs2, the biochemical assays and the EM analysis are detailed in Methods.

Supplementary Material

Refer to Web version on PubMed Central for supplementary material.

Acknowledgments

We thank M. Alexeeva for the cell culture support. We thank P. Sung, R. Kolodner, and L. Symington for plasmids and yeast strains. We are grateful to S. Kowalczykowski, N. Hunter, D. Castaño-Diez, P. Ringler and all members of the Heyer laboratory for discussions and comments on the manuscript. This work was supported by a Postdoctoral fellowship 17FT-0046 from the Tobacco-Related Disease Research Program (J.L.), by European Community (LSHG-CT-2003-503303) and the Centre National de la Recherche Scientifique, the Commissariat à l'Énergie Atomique (X.V., F.F.), by SystemsX.ch (H.S.), the National Institutes of Health (NIH) U54GM74929 (H.S.) and CA92267 and GM58015 (W.D.H.).

References

1. Heyer WD, Ehmsen KT, Liu J. Regulation of homologous recombination in eukaryotes. *Annu Rev Genet.* 2010; 44:113–139. [PubMed: 20690856]
2. Symington LS. Role of *RAD52* epistasis group genes in homologous recombination and double-strand break repair. *Microbiol Mol Biol Rev.* 2002; 66:630–670. [PubMed: 12456786]
3. Thacker J. The RAD51 gene family, genetic instability and cancer. *Cancer Lett.* 2005; 219:125–135. [PubMed: 15723711]
4. Sung P. Yeast Rad55 and Rad57 proteins form a heterodimer that functions with replication protein A to promote DNA strand exchange by Rad51 recombinase. *Genes Dev.* 1997; 11:1111–1121. [PubMed: 9159392]
5. Lovett ST, Mortimer RK. Characterization of null mutants of the *RAD55* gene of *Saccharomyces cerevisiae*: Effects of temperature, osmotic strength and mating type. *Genetics.* 1987; 116:547–553. [PubMed: 3305159]
6. Beernink HTH, Morrical SW. RMPs: Recombination/replication mediator proteins. *Trends Biochem Sci.* 1999; 24:385–389. [PubMed: 10500302]
7. Morimatsu K, Kowalczykowski SC. RecFOR proteins load RecA protein onto gapped DNA to accelerate DNA strand exchange: A universal step of recombinational repair. *Mol Cell.* 2003; 11:1337–1347. [PubMed: 12769856]
8. Liu J, Doty T, Gibson B, Heyer WD. Human BRCA2 protein promotes RAD51 filament formation on RPA-covered single-stranded DNA. *Nat Struct Mol Biol.* 2010; 17:1260–1262. [PubMed: 20729859]
9. Jensen RB, Carreira A, Kowalczykowski SC. Purified human BRCA2 stimulates RAD51-mediated recombination. *Nature.* 2010; 467:678–683. [PubMed: 20729832]
10. Lisby M, Barlow JH, Burgess RC, Rothstein R. Choreography of the DNA damage response: Spatiotemporal relationships among checkpoint and repair proteins. *Cell.* 2004; 118:699–713. [PubMed: 15369670]

11. Schiestl RH, Prakash S, Prakash L. The *SRS2* suppressor of *rad6* mutations of *Saccharomyces cerevisiae* acts by channeling DNA lesions into the *RAD52* DNA repair pathway. *Genetics*. 1990; 124:817–831. [PubMed: 2182387]
12. Aboussekhra A, et al. *RADH*, a gene of *Saccharomyces cerevisiae* encoding a putative DNA helicase involved in DNA repair. Characteristics of *radH* mutants and sequence of the gene. *Nucleic Acids Res*. 1989; 17:7211–7219. [PubMed: 2552405]
13. Aguilera A, Klein HL. Genetic control of intrachromosomal recombination in *Saccharomyces cerevisiae*. I. Isolation and genetic characterization of hyper-recombination mutations. *Genetics*. 1988; 119:779–790. [PubMed: 3044923]
14. Krejci L, et al. DNA helicase Srs2 disrupts the Rad51 presynaptic filament. *Nature*. 2003; 423:305–309. [PubMed: 12748644]
15. Veaute X, et al. The Srs2 helicase prevents recombination by disrupting Rad51 nucleoprotein filaments. *Nature*. 2003; 423:309–312. [PubMed: 12748645]
16. Antony E, et al. Srs2 Disassembles Rad51 Filaments by a Protein-Protein Interaction Triggering ATP Turnover and Dissociation of Rad51 from DNA. *Mol Cell*. 2009; 35:105–115. [PubMed: 19595720]
17. Dupaigne P, et al. The Srs2 helicase activity is stimulated by Rad51 filaments on dsDNA: Implications for crossover incidence during mitotic recombination. *Mol Cell*. 2008; 29:243–254. [PubMed: 18243118]
18. Hilario J, Amitani I, Baskin RJ, Kowalczykowski SC. Direct imaging of human Rad51 nucleoprotein dynamics on individual DNA molecules. *Proc Nat Acad Sci USA*. 2009; 106:361–368. [PubMed: 19122145]
19. Modesti M, et al. Fluorescent human RAD51 reveals multiple nucleation sites and filament segments tightly associated along a single DNA molecule. *Structure*. 2007; 15:599–609. [PubMed: 17502105]
20. Fung CW, Mozlin AM, Symington LS. Suppression of the Double-Strand-Break-Repair defect of the *Saccharomyces cerevisiae rad57* mutant. *Genetics*. 2009; 181:1195–1206. [PubMed: 19189942]
21. Herzberg K, et al. Phosphorylation of Rad55 on serines 2, 8, and 14 is required for efficient homologous recombination in the recovery of stalled replication forks. *Mol Cell Biol*. 2006; 26:8396–8409. [PubMed: 16966380]
22. Saponaro M, et al. Cdk1 Targets Srs2 to Complete Synthesis-Dependent Strand Annealing and to Promote Recombinational Repair. *Plos Genetics*. 2010; 6:e1000858. [PubMed: 20195513]
23. Papouli E, et al. Crosstalk between SUMO and ubiquitin on PCNA is mediated by recruitment of the helicase Srs2p. *Mol Cell*. 2005; 19:123–133. [PubMed: 15989970]
24. Pfander B, Moldovan GL, Sacher M, Hoege C, Jentsch S. SUMO-modified PCNA recruits Srs2 to prevent recombination during S phase. *Nature*. 2005; 436:428–433. [PubMed: 15931174]
25. Burgess RC, et al. Localization of recombination proteins and Srs2 reveals anti-recombinase function in vivo. *J Cell Biol*. 2009; 185:969–981. [PubMed: 19506039]
26. Meindl A, et al. Germline mutations in breast and ovarian cancer pedigrees establish RAD51C as a human cancer susceptibility gene. *Nature Gen*. 2010; 42:410–414.
27. Hu Y, et al. RECQL5/Recql5 helicase regulates homologous recombination and suppresses tumor formation via disruption of Rad51 presynaptic filaments. *Genes Dev*. 2007; 21:3073–3084. [PubMed: 18003859]
28. Bugreev DV, Yu X, Egelman EH, Mazin AV. Novel pro- and anti-recombination activities of the Bloom's syndrome helicase. *Genes Dev*. 2007; 21:3085–3094. [PubMed: 18003860]
29. Sommers JA, et al. FANCD1 uses its motor ATPase to destabilize protein-DNA complexes, unwind triplexes, and inhibit RAD51 strand exchange. *J Biol Chem*. 2009; 284:7502–7514.
30. Fugger K, et al. Human Fbh1 helicase contributes to genome maintenance via pro- and anti-recombinase activities. *J Cell Biol*. 2009; 186:655–663. [PubMed: 19736316]

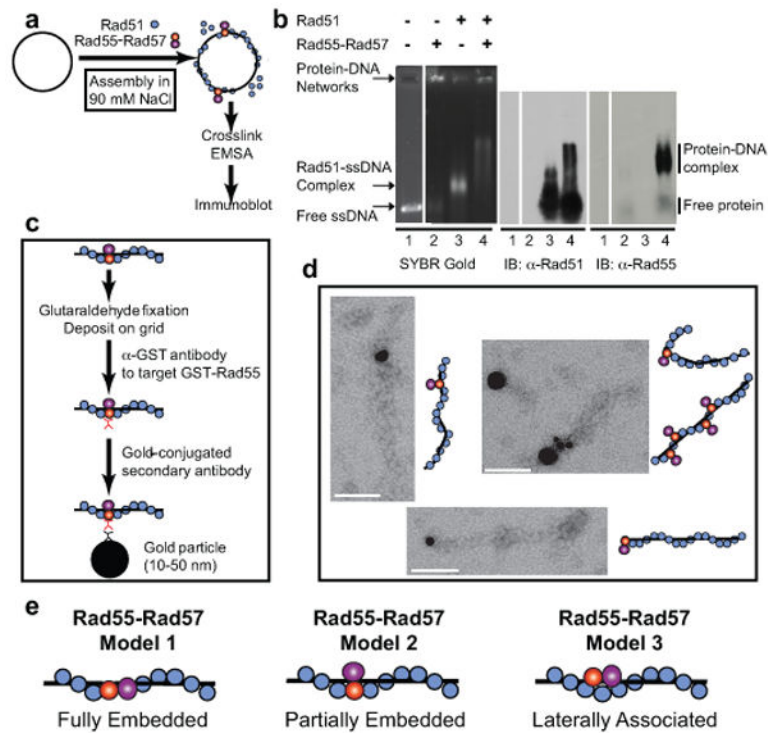


Figure 1. Rad55-Rad57 is associated with and stabilizes Rad51-ssDNA filaments

a, Rad51-ssDNA filament assembly assay. **b**, $0.67 \mu\text{M}$ Rad51 \pm $0.11 \mu\text{M}$ Rad55-Rad57 was incubated with $4 \mu\text{M}$ ϕX174 ssDNA. The migration position of free protein was confirmed in controls lacking DNA (Supplementary Fig. 3c). **c**, Reaction scheme of immunogold labeling of Rad55. **d**, EM images of gold-labeled Rad55 associated with Rad51-ssDNA filament (1:3 Rad51/nucleotide; $2.34 \mu\text{M}$ Rad51 \pm $0.43 \mu\text{M}$ Rad55-Rad57, $7 \mu\text{M}$ (nt) ssDNA). Scale bars: 100 nm. **e**, Models for the disposition of Rad55-Rad57 with the Rad51 filament. For simplicity, only model 2 is drawn in all illustrations.

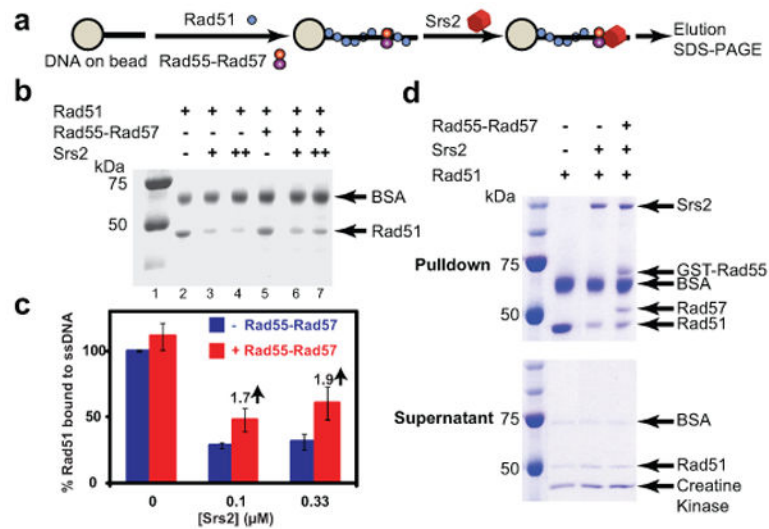


Figure 2. Rad55-Rad57 stabilizes Rad51-ssDNA filaments to resist disruption by Srs2
a, Pull-down assay measuring stability of Rad51-ssDNA complexes (1 Rad51: 3 nt, 1 μM Rad51 ± 0.1 μM Rad55-Rad57) against disruption by Srs2 (0.1 or 0.33 μM). **b**, Rad51 remaining bound to ssDNA. **c**, Quantitation of results in (b) and additional experiments. Shown are means ± 1 sd, n=3. **d**, Concomitant binding of Rad55-Rad57 and Srs2 to Rad51-covered ssDNA. Pull-down assay measuring stability of Rad51-ssDNA complexes (1 Rad51: 3 nt, 1 μM Rad51 ± 0.2 μM Rad55-Rad57) against disruption by 0.33 μM Srs2. Top, pull-downs; bottom, supernatants.

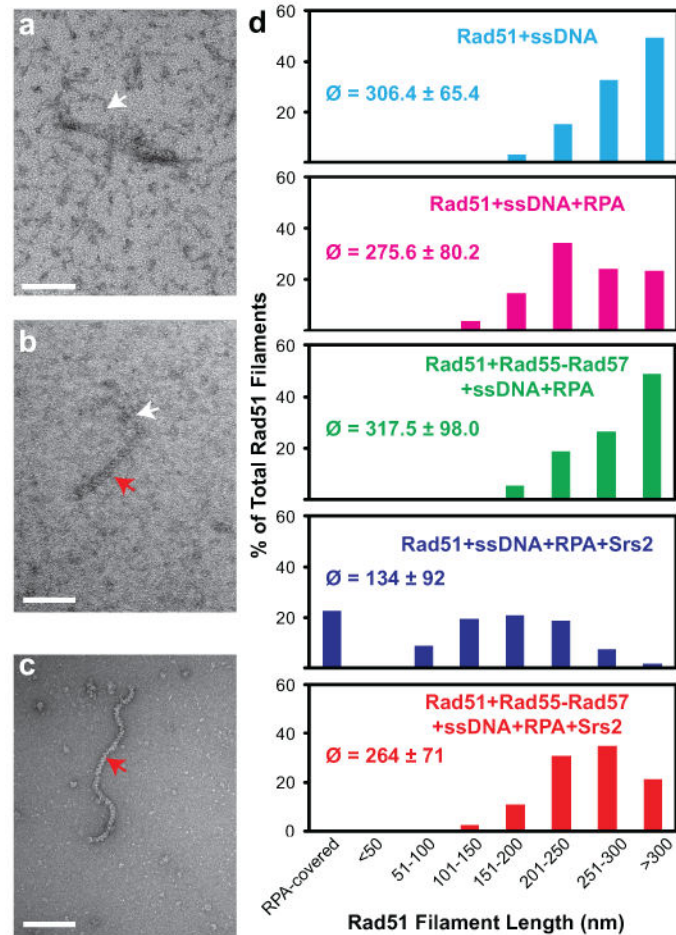


Figure 3. Rad55-Rad57 inhibit disruption of Rad51 presynaptic filaments by Srs2
a, RPA-ssDNA complex. **b**, Short (145 nm) Rad51-ssDNA filament. **c**, Long (350 nm) Rad51-ssDNA filaments **d**, Quantitation of electron microscopic analysis. 300-400 filaments were analyzed for each reaction condition (2.34 μ M Rad51, 7 μ M (nt) 600 nt ssDNA, \pm 0.43 μ M Rad55-Rad57, \pm 0.21 μ M RPA, \pm 0.4 μ M Srs2), and the means (ϕ) \pm 1 sd and distributions of filament length classes are shown. Scale bars: 100 nm. White arrows indicate RPA-ssDNA complexes and red arrows Rad51 filaments.

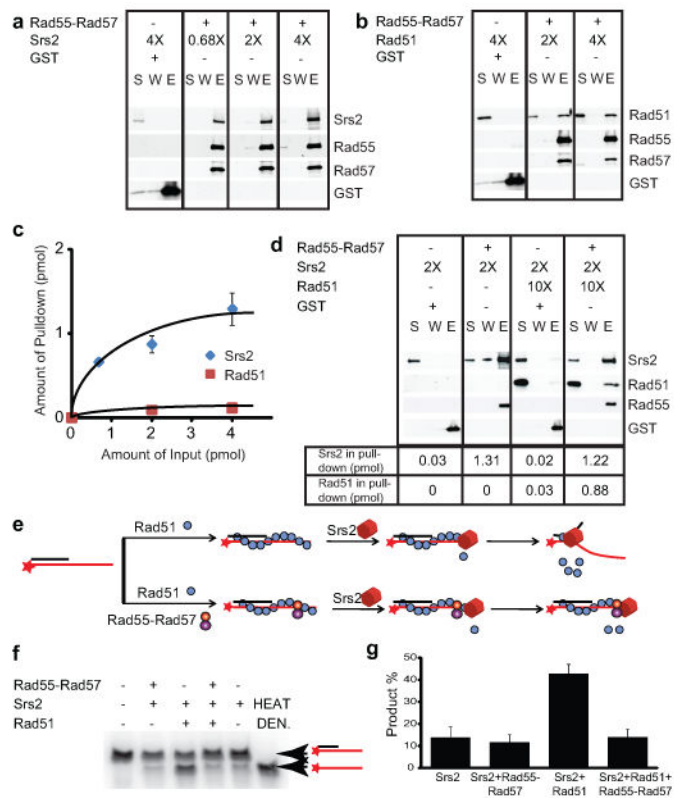


Figure 4. Rad55-Rad57 interact with Srs2 and inhibit Srs2 helicase

a, Pull-down with 4 nM (1 pmol) Rad55-Rad57 and 2.7, 8, or 16 nM Srs2. **b**, Pull-down with 4 nM Rad55-Rad57 and 8 or 16 nM Rad51. **c**, Quantitation of results in (a) and (b) and additional experiments. **d**, Pull-down with 4 nM Rad55-Rad57 and 8 nM Srs2 \pm 40 nM Rad51. GST was used as control. S: supernatant, W: wash, E: eluate. **e**, Helicase assay. **f**, 28 nM Rad51 \pm 25 nM Rad55-Rad57 were incubated with 1.5 nM 3'-tailed substrate before addition of 120 nM Srs2 protein. Product yields at 20 min. were quantified as shown in **g**. HEAT DEN.: heat denatured substrate, shown are means \pm 1sd, n=3.